

Original Article



Metabolomic Profiling Differences among Asthma, COPD, and Healthy Subjects: A LC-MS-based Metabolomic Analysis*

LIANG Ying^{1,&}, GAI Xiao Yan^{1,&}, CHANG Chun^{1,#}, ZHANG Xu², WANG Juan³, and LI Ting Ting⁴

1. Department of Pulmonary and Critical Care Medicine, Peking University Third Hospital, Beijing 100191, China; 2. Tianjin Key Lab. of Metabolic Diseases and Department of Physiology, Tianjin Medical University, Tianjin 300070, China; 3. Lab. of Respiratory Disease, Peking University Third Hospital, Beijing 100191, China; 4. Department of Biomedical Informatics, School of Basic Medical Sciences, Peking University Health Science Centre, Beijing 100191, China

Abstract

Objective Asthma and chronic obstructive pulmonary disease (COPD) feature different inflammatory and cellular profiles in the airways, indicating that the cellular metabolic pathways regulating these disorders are distinct.

Methods We aimed to compare the serum metabolomic profiles among mild persistent asthmatic patients, individuals with stable COPD, and healthy subjects and to explore the potential metabolic biomarkers and pathways. The serum metabolomic profiles of 17 subjects with mild persistent asthma, 17 subjects with stable COPD, and 15 healthy subjects were determined by an untargeted metabolomic analysis utilizing liquid chromatography-mass spectrometry. A series of multivariate statistical analyses was subsequently used.

Results Multivariate analysis indicated a distinct separation between the asthmatic patients and healthy controls in electrospray positive and negative ions modes, respectively. A total of 19 differential metabolites were identified. Similarly, a distinct separation between asthma and COPD subjects was detected in the two ions modes. A total of 16 differential metabolites were identified. Among the identified metabolites, the serum levels of hypoxanthine were markedly higher in asthmatic subjects compared with those in COPD or healthy subjects.

Conclusions Patients with asthma present a unique serum metabolome, which can distinguish them from individuals with COPD and healthy subjects. Purine metabolism alteration may be distinct and involved in the pathogenesis of asthma.

Key words: Asthma; Chronic obstructive pulmonary disease; Metabolomics; Liquid chromatography; Mass spectrometry

Biomed Environ Sci, 2019; 32(9): 659-672 doi: 10.3967/bes2019.085 ISSN: 0895-3988

www.besjournal.com (full text) CN: 11-2816/Q Copyright ©2019 by China CDC

*This research was funded by the National Natural Science Foundation of China-Youth Fund Project [No. 81400017, 81700039, 81800038]; and the National Natural Science Foundation of China Emergency Management Project [No. 81641153].

&These authors contributed equally to this work.

#Correspondence should be addressed to CHANG Chun, Tel: 86-15810075362, E-mail: doudou_1977@163.com

Biographical notes of the first authors: LIANG Ying, male, born in 1982, MD, Associated Chief Physician, majoring in COPD, asthma, respiratory critical illness; GAI Xiao Yan, female, born in 1981, MD, Attending Doctor, majoring in COPD, asthma.

INTRODUCTION

Asthma is a disease that affects 1%-18% of the human population worldwide. Asthma is heterogeneous and characterized by various symptoms and reversible expiratory airflow limitation^[1,2]. Given the heterogeneity of underlying pathogenesis and variety of respiratory symptoms, the early diagnosis and management of asthma are considerably difficult, notably in asthmatic children^[3,4]. Chronic obstructive pulmonary disease (COPD) is another common chronic respiratory disease characterized by persistent respiratory symptoms and irreversible airflow limitation^[5,6]. In clinical practice, differential diagnosis between these diseases is sometimes difficult due to the similar clinical presentations and lung function test results^[7].

The pathogenesis and pathology of asthma differ from those of COPD, involving the different inflammatory cells and inflammatory mediators in the airways^[8]. COPD is characterized by the increased number of macrophages in the peripheral airways, lung parenchyma, pulmonary vessels, and activated neutrophils and lymphocytes, such as T-helper (Th) 1 and Th17 cells^[6]. Asthma is characterized by the increased number of activated eosinophils, mast cells, and Th2 lymphocytes in the airways, together with the increased levels of inflammatory mediators, such as interleukin-4 and 5^[1]. The diagnosis of asthma or COPD is mainly based on patient clinical symptoms and spirometry function testing. Invasive diagnostic methods, including bronchoscopy and surgery, can improve the diagnostic accuracy^[9] but are unnecessary for every patient due to their invasive characteristics. Nevertheless, non-invasive diagnostic approaches that can be used to distinguish asthma from COPD are still limited.

Metabolomics is the comprehensive assessment of low-molecular-weight (< 1,000 Da) endogenous metabolites; it can reflect the biochemical reactions and metabolic changes under a given set of physiological or pathophysiological conditions^[10]. Endogenous metabolites include a wide variety of small molecules, such as sugars, lipids, steroids, and amino acids^[11]. These metabolites represent the functional phenotypes of a cell, tissue, or organism^[12]. Currently, metabolomics, which is non-invasive and can be applied to various types of biological fluids, has been deemed considerably helpful for the identification of metabolites related to the diagnosis and prognosis of diseases and can

provide early disease detection and deep understanding of disease pathogenesis^[13]. In the past decade, both mass spectrometry (MS)^[14-17] and nuclear magnetic resonance (NMR)^[18-24]-based metabolomic techniques have been utilized in the diagnosis of asthma and have demonstrated evident metabolic alterations associated with the pathogenesis of this disease. Moreover, our previous pilot study has shown that serum metabolic activity is significantly altered in patients with mild persistent asthma based on gas chromatography (GC) coupled with MS^[25]. However, the differences in metabolic profiling of serum samples among asthmatic, COPD, and healthy individuals have not been previously studied by liquid chromatography (LC) coupled with MS methodologies. This innovative method can provide the complementary detection of high-molecular-weight metabolites with poor thermal stability that cannot be detected by GC-MS^[26].

In the present study, we applied a LC-MS method on the serum samples derived from patients with asthma and COPD and healthy subjects and investigated the metabolomic alteration and differences among these groups. We hypothesized that the metabolic profiling of asthmatic patients differs from that of COPD or healthy subjects and that LC-MS-based metabolomic analysis could assist clinicians to distinguish asthma from COPD.

METHODS

Study Subjects

A total of 17 patients with mildly persistent asthma, 17 patients with stable COPD, and 15 healthy subjects were recruited from the respiratory clinic of the Peking University Third Hospital between January 2015 and December 2016. Asthma was diagnosed according to the Global Initiative for Asthma guidelines. COPD was diagnosed according to the Global Initiative for Chronic Obstructive Lung Disease guidelines. The healthy subjects had no history or appearance of chronic respiratory diseases or other diseases that might influence the results. The subjects' clinical data, including demographic characteristics, tobacco exposure, blood glucose, blood triglyceride and cholesterol, and spirometry function, were collected. These data were analyzed anonymously in our study.

The exclusion criteria were the following: subjects with airflow limitation diseases other than asthma or COPD; acute exacerbation of asthma or

COPD within the prior four weeks; any other acute infection or sepsis within the same time period; definite neoplastic diseases; severe trauma or surgery within the same time period.

All the study subjects participating in the present study had provided informed consent prior to data collection. The present study was performed in accordance with the Declaration of Helsinki (1964) and all subsequent revisions and approved by the Ethics Committee of Peking University Third Hospital (2014071).

Serum Sample Collection

To avoid and minimize the variation in the biochemical parameters due to circadian rhythms, blood samples were collected in the morning between 8:00 AM and 10:30 AM following overnight fasting (at least 8 h). Blood samples were transferred into serum gel tubes and gently inverted twice. The samples were allowed to rest at room temperature for 30 min until complete coagulation. The tubes were centrifuged at 2,500 $\times g$ for 15 min at 4 °C. The serum was immediately divided into aliquots, transferred in cryovials, and stored at -80 °C for further analysis.

Statistical Analysis

The demographic characteristics of the study subjects were analyzed by the SPSS software (version 19.0, IBM, Armonk, NY, USA). Continuous variables were expressed as mean \pm standard deviation, and categorical variables were expressed as numbers. The *t*-test was used to assess the differences among groups considering continuous variables. The chi-squared test was used for assessment of the differences in categorical variables. The results were considered statistically significant at *P*-values lower than 0.05 (*P* < 0.05).

LC-MS Analysis

Sample Preparation Each 100 μ L aqueous serum was added to 400 μ L methanol-acetonitrile (1:1, vol/vol) solution and vortexed for 30 s. Following incubation for 1 h at -20 °C, the mixed sample was centrifuged at 12,000 rpm at 4 °C for 15 min. Subsequently, 400 μ L supernatant was isolated and evaporated to dryness at room temperature. The dried residue was reconstituted in 100 μ L acetonitrile-H₂O (1:1, vol/vol). Following sonication for 10 min in a water bath and centrifugation for 15 min at 12,000 rpm at 4 °C, the supernatant was isolated and kept at -80 °C prior to LC-MS analysis. The quality control (QC) sample was derived from

small aliquots of all the studied samples, which were pooled and thoroughly mixed, and then processed in the same way as the studied samples.

Detection Platform And Validation LC-MS analysis was performed using an Agilent 1290 ultraperformance liquid chromatography (UPLC) system (Agilent Technologies, Santa Clara, CA, USA) coupled with an AB Triple quadrupole time-of-flight 5,600 mass spectrometer (AB SCIEX, Foster City, CA, USA). The system utilized ACQUITY UPLC BEH Amide (2.1 mm \times 100 mm, 1.7 μ m, Waters, USA) as the chromatographic column.

A total of 10 μ L of each reconstituted sample was obtained from sample vials, which were stored at 4 °C, and injected onto the UPLC column. Chromatographic separations utilized a binary mobile phase system (phase A: water containing 25 mmol/L ammonium acetate and 25 mmol/L ammonium hydroxide; phase B: acetonitrile). Gradient elution was performed as described in [Supplementary Table 1](#) (www.besjournal.com). The eluent from the column was directed to MS analysis without split. The QC sample was injected on the column randomly. Six replicates of QC sample were used for the evaluation of the method reproducibility.

An electrospray ionization source (ESI) operating in positive and negative ion modes was used in MS analysis, with spraying voltage of 5.5 kV for ESI+ mode and of -4.5 kV for ESI- mode. The ionization temperature was set at 600 °C. The voltages of atomization gas, auxiliary gas, and curtain gas were set at 60, 60, and 35 psi, respectively. The declustering potential was set at 60 V, and the range of collision energy was set at 35 \pm 15 eV. The data were collected in the centroid mode form with a *m/z* range of 60 to 1,200.

LC-MS Data Analysis

Data Pre-processing And QC The analysis conducted in 49 serum samples resulted in the detection of 16,262 peaks in the ESI+ mode, whereas 13,983 peaks were detected in the ESI-mode. The open-source XCMS software package (Version xcms4dda) was used to process raw data. The XCMS settings were the following: S/N threshold, 6; accurate molecular weight deviation, 25; peak width, 5-30 s. Following the acquisition of a matrix, the metabolite features with associated retention time (RT), accurate mass, and chromatographic peak area and data alignment and normalization were performed using QC samples. The metabolic features with poor reproducibility were removed.

Normalization was processed by the total ion current. The total area normalization method was performed on this data analysis set. The reproducibility of the method was assessed by the internal standard response stability, the dispersion of QC samples in principal component analysis (PCA) scatter plot (Supplementary Figures S1-S4 available in www.besjournal.com), and the correlation among the QC samples. Finally, 2,446 peaks were identified in the ESI+ mode, and 1,761 peaks in the ESI- mode were reserved and subjected to further multivariate analysis.

Multivariate Analysis The three-dimensional (3D) data involving the peak number, sample name, and normalized peak area were processed with the SIMCA 14.0 software package (Umetrics AB, Umea, Sweden) for PCA and orthogonal projections to latent structures-discriminate analysis (OPLS-DA). PCA indicated the distribution of the origin data. To obtain a higher level of group separation and a better understanding of the variables responsible for classification, supervised OPLS-DA was applied. To refine this analysis, the first principal component of the variable importance projection (VIP) was obtained. The Student's *t*-test was used for pairwise comparison. The VIP values exceeding 1.0 with a *P*-value lower than 0.05 ($P < 0.05$) in the Student's *t*-test were selected to correspond to potential differential metabolites.

Metabolite Identification, Receiver Operating Characteristic (ROC) Curve, And Pathway Analysis

The selected differential metabolites were further identified by searching the Kyoto Encyclopedia of Genes and Genomes (KEGG), the METLIN databases for first-order MS, and a self-built database for second-order MS. The ROC curves were determined, and the area under the ROC curve (AUC) was used to detect the efficiency of this method in distinguishing asthma from healthy subjects or COPD patients. Finally, each potential differential metabolite was cross-listed with the metabolic pathways in the KEGG database. The top altered metabolic pathways were then identified and constructed to relevant reference maps.

RESULTS

Subject Characteristics

The patients with COPD were older than those with asthma and healthy subjects. The ages between asthma and healthy controls were comparable. The sex proportions showed no statistical difference

among the three groups ($P = 0.224$). The patients with COPD included 2 current smokers (11.8%), 10 ex-smokers (58.8%), and 5 non-smokers (29.4%). Neither patients with asthma nor healthy subjects were smokers. Similar levels of blood glucose, triglyceride, and cholesterol were observed among the three groups. The patients with COPD exhibited the worst spirometry function among the three groups (Table 1).

Metabolomic Profiling Differences between Asthmatic Patients and Healthy Subjects

Data In Electrospray Positive Ion Mode As shown in Figure 1A, PCA indicated a distinct separation between the asthma and healthy subjects, and the majority of the samples were within the 95% confidence interval (*CI*) with the exception of those corresponding to two asthmatic patients. The OPLS-DA plot further showed distinct separation between the asthmatic and healthy subjects (Figure 1B). Similarly, the majority of the samples were within the 95% *CI* with the exception of one asthmatic sample. The R^2Y and Q^2Y of this OPLS-DA model were 0.994 and 0.980, respectively.

Data In Electrospray Negative Ion Mode As shown in Figure 2A, PCA also demonstrated a distinct separation between asthma and healthy subjects, and the majority of the samples were within the 95% *CI* with the exception of one sample corresponding to an asthmatic patient. The OPLS-DA plot indicated the distinct separation between the asthmatic patients and healthy subjects (Figure 2B). Similarly, the majority of the samples were within the 95% *CI*, with the exception of two samples from the asthmatic patients. The R^2Y and Q^2Y of this OPLS-DA model were 0.991 and 0.921, respectively.

Identification Of Differential Levels Of Metabolites

Based on the score, the VIP, and *P*-value, we identified 5 different metabolites in the ESI+ mode and 14 different metabolites in the ESI- mode (Table 2). In the ESI+ mode, the levels of hypoxanthine, *p*-chlorophenylalanine, and inosine significantly increased in the asthmatic patients, whereas the levels of L-glutamine and glycerophosphocholine significantly decreased compared with the control subjects. In the ESI- mode, the levels of hypoxanthine, theophylline, bilirubin, inosine, and palmitic acid were significantly higher in the asthmatic patients compared with those in COPD subjects, whereas the levels of succinate, xanthine, arachidonic acid, L-pyrogutamic acid, indoxyl sulfate, L-valine, L-norleucine, L-leucine, and L-phenylalanine were significantly lower in the

asthmatic patients compared with control subjects. The ROC curve was used to evaluate the predictive performance of the aforementioned differential metabolites. Figure 3 shows the metabolites with $AUC \geq 0.8$.

Metabolomic Profiling Difference between the Asthmatic and COPD Subjects

Data in Electrospray Positive Ion Mode PCA

roughly detected a differential metabolic profile between asthma and COPD (Figure 4A). One sample corresponding to an asthmatic patient was outside the 95% CI. Based on the OPLS-DA, the score scatter plot indicated a clear separation between the asthmatic and COPD (Figure 4B) subjects, and all the samples were within the 95% CI. The R^2Y and Q^2Y values in this OPLS-DA model were 0.879 and 0.252, respectively.

Table 1. Demographic characteristics of the study subjects

Characteristics	Asthma (n = 17)	COPD (n = 17)	Controls (n = 15)
Age (year)	53.7 ± 19.5	79.3 ± 8.8 ^{††}	48.5 ± 12.9
Male/Female	6/11	11/6	8/7
Height (cm)	169.6 ± 6.7	173.7 ± 4.7	171.3 ± 3.9
Weight (kg)	67.6 ± 5.8	67.4 ± 5.2	66.5 ± 3.8
BMI (kg/m ²)	23.5 ± 1.6	22.3 ± 1.2	22.7 ± 1.2
Smoking status			
Current-	0	2	0
Ex-	0	10	0
Never-	17	5	15
Glucose (mmol/L)	4.9 ± 0.7	4.8 ± 0.8	4.6 ± 0.8
Triglyceride (mmol/L)	1.8 ± 0.3	1.8 ± 0.3	1.7 ± 0.3
Total cholesterol (mmol/L)	4.1 ± 0.8	4.0 ± 0.7	4.2 ± 0.9
High density lipoprotein (mmol/L)	1.5 ± 0.6	1.6 ± 0.5	1.6 ± 0.5
Low density lipoprotein (mmol/L)	2.4 ± 0.5	2.7 ± 0.9	2.8 ± 1.0
FEV1/FVC (%)	79.4 ± 4.2	61.3 ± 6.3 ^{††}	86.0 ± 4.7
FEV1 %predicted	89.9 ± 4.0 [*]	59.6 ± 6.8 ^{††}	91.5 ± 4.4

Note. [†] COPD vs. Asthma, $P < 0.001$; [‡] COPD vs. Controls, $P < 0.001$; ^{*} Asthma vs. Controls, $P < 0.001$.

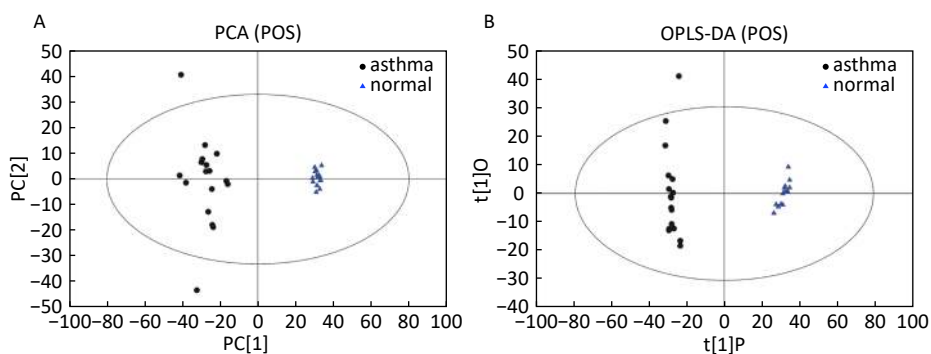


Figure 1. PCA and OPLS-DA of LC-MS metabolite profiles between asthmatic and healthy subjects based on the electrospray positive ion mode. (A) Score scatter plot of PCA model obtained from asthmatic and healthy subjects. The X-(PC[1]) and Y-axis (PC[2]) indicate the first and second principal components, respectively. (B) Score scatter plot of the OPLS-DA model obtained from the asthmatic and healthy subjects. The X-(t[1]P) and Y-axis (t[1]O) indicate the predictive and orthogonal directions, respectively. PCA: principal component analysis; OPLS-DA: orthogonal projections to latent structures-discriminate analysis; LC-MS: liquid chromatography-mass spectrometry.

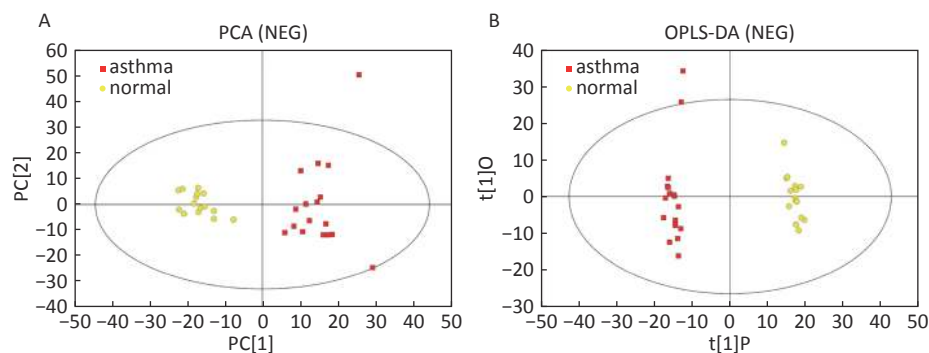


Figure 2. PCA and OPLS-DA of LC-MS metabolite profiles between the asthmatic and healthy subjects in electrospray negative ion mode. (A) Score scatter plot of PCA model obtained from asthmatic and healthy subjects. The X-(PC[1]) and Y-axis (PC[2]) indicate the first and second principal components, respectively. (B) Score scatter plot of the OPLS-DA model obtained from the asthmatic and healthy subjects. The X-(t[1]P) and Y-axis (t[1]O) indicate the predictive and orthogonal directions, respectively. PCA: principal component analysis; OPLS-DA: orthogonal projections to latent structures-discriminate analysis; LC-MS: liquid chromatography-mass spectrometry.

Table 2. Differentially expressed metabolites between asthmatic and healthy subjects

Metabolite name	Score	Median RT (s)	Mean asthma	Mean control	VIP	P-value	Fold-change ^a
Positive ion mode (ESI+)							
Hypoxanthine	0.888	127.044	762,120.978	107,680.398	1.292	1.828×10^{-6}	7.078
P-chlorophenylalanine	0.946	299.633	103,213.840	69,289.675	1.082	3.215×10^{-5}	1.490
L-Glutamine	0.951	386.792	14,215.705	52,805.785	1.329	2.179×10^{-6}	0.269
Glycerophosphocholine	0.990	473.276	107,868.019	432,953.058	1.331	1.876×10^{-6}	0.249
Inosine	0.997	172.638	402,568.442	21,353.459	1.262	3.141×10^{-6}	18.853
Negative ion mode (ESI-)							
Hypoxanthine	0.986	127.177	421,202.385	58,594.857	1.993	2.494×10^{-6}	7.188
Succinate	0.986	467.769	24,293.468	30,744.437	1.155	9.328×10^{-3}	0.790
Xanthine	0.997	170.712	69,038.696	145,934.844	1.988	6.556×10^{-6}	0.473
Arachidonic Acid (peroxide free)	0.950	46.921	550,848.247	1408,228.636	1.896	4.184×10^{-5}	0.391
L-Pyroglutamic acid	0.998	267.481	419,335.669	722,668.930	1.609	2.727×10^{-4}	0.580
Indoxyl sulfate	0.996	46.881	253,902.424	399,864.278	1.146	1.160×10^{-2}	0.635
Theophylline	0.969	63.751	746,404.311	27,458.526	1.143	5.567×10^{-3}	27.183
L-Valine	0.990	283.093	238,204.741	329,407.691	1.643	1.128×10^{-4}	0.723
L-Norleucine	0.992	212.926	611,132.345	862,255.499	1.571	2.653×10^{-4}	0.709
Bilirubin	0.997	54.940	16,581.417	9,240.124	1.050	3.550×10^{-2}	1.795
L-Leucine	0.997	234.501	551,017.884	780,835.022	1.387	1.354×10^{-3}	0.706
Inosine	0.998	171.190	841,330.913	31,156.248	1.799	3.193×10^{-5}	27.004
Palmitic acid	0.999	161.731	116,896.629	79,641.247	1.329	3.144×10^{-3}	1.468
L-Phenylalanine	0.919	197.371	527,761.313	683,438.123	1.589	4.118×10^{-4}	0.772

Note. ^aFold-change: Asthma versus Control. Abbreviations: RT: retention time; VIP: variable importance for the projection.

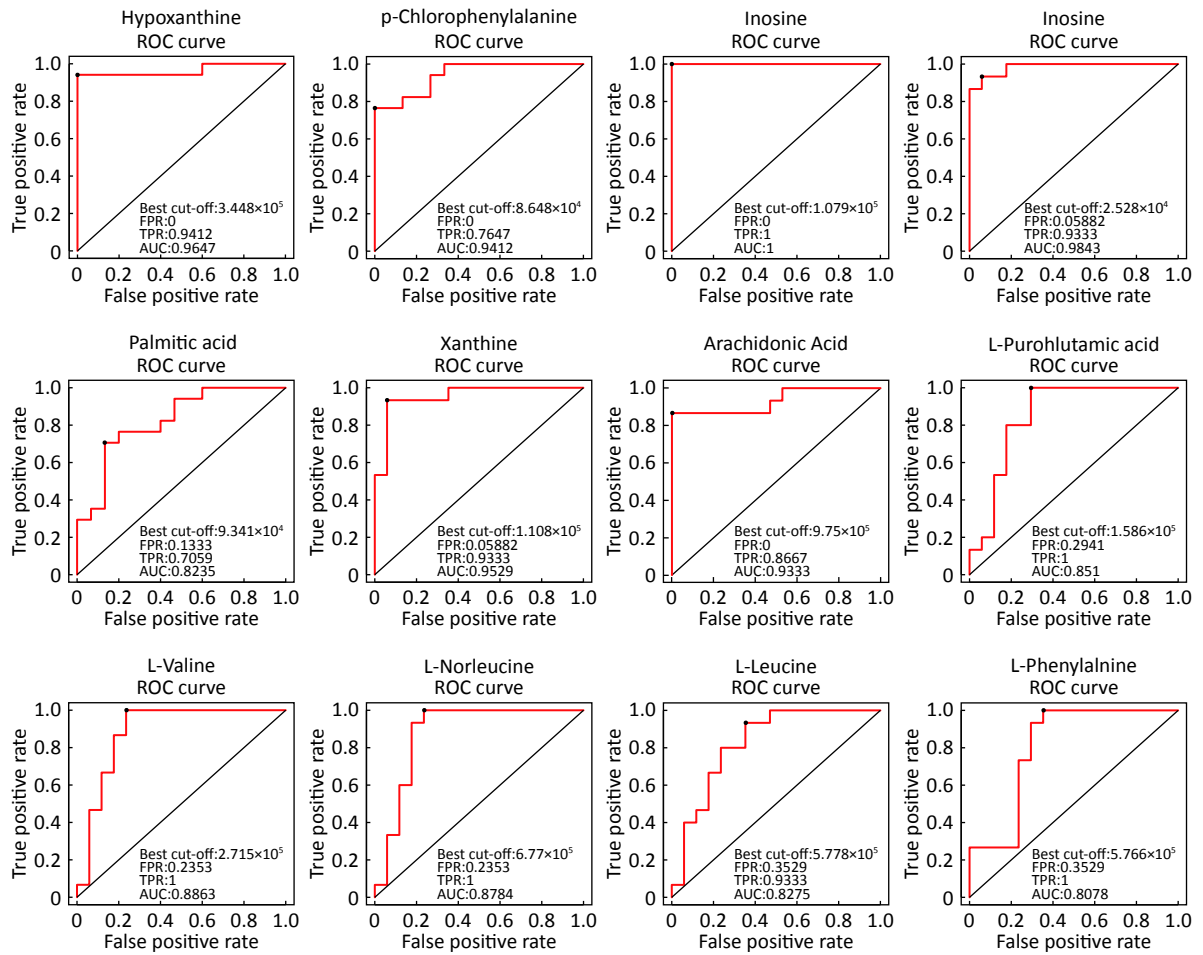


Figure 3. ROC curves of differential metabolites between asthmatic and control subjects with AUC \geq 0.80.

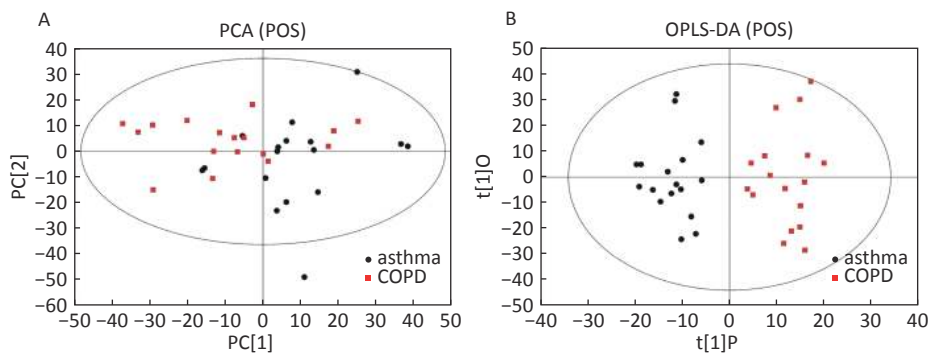


Figure 4. PCA and OPLS-DA of LC-MS metabolite profiles between the asthmatic and COPD subjects in electrospray positive ion mode. (A) Score scatter plot of PCA model obtained from the asthma and COPD subjects. The X-(PC[1]) and Y-axis (PC[2]) indicate the first and second principal components, respectively. (B) Score scatter plot of the OPLS-DA model obtained from asthmatic and COPD subjects. The X-(t[1]P) and Y-axis (t[1]O) indicate the predictive and orthogonal directions, respectively. PCA: principal component analysis; OPLS-DA: orthogonal projections to latent structures-discriminate analysis; LC-MS: liquid chromatography-mass spectrometry; COPD: chronic obstructive pulmonary disease.

Data in Electrospray Negative Ion Mode The trends of sample distribution also differed between the asthmatic and COPD subjects in PCA (Figure 5A). One sample that corresponded to an asthmatic patient was outside the 95% CI. OPLS-DA indicated a straightforward separation between the asthma and COPD patients, and one asthmatic sample was outside the 95% CI (Figure 5B). The R^2Y and Q^2Y values in this OPLS-DA model were 0.901 and 0.252, respectively.

Identification of Metabolite Differential Levels

Based on the score, VIP, and P -values, we detected nine different metabolites in the ESI+ mode and seven different metabolites in ESI- mode (Table 3). In the ESI+ mode, the levels of hypoxanthine, L-pipecolic acid, p-chlorophenylalanine, and acetylcarnitine were significantly higher in the asthmatic patients, whereas the levels of alpha-N-phenylacetyl-L-glutamine, 1-methyladenosine, glycochenodeoxycholate, L-citrulline, and L-glutamine were significantly decreased in asthmatic patients compared with those of the COPD patients. In the ESI- mode, the levels of linoleic acid and hypoxanthine were significantly higher in asthmatic patients, whereas the levels of pseudouridine, alpha-N-phenylacetyl-L-glutamine, succinate, L-citrulline, and glycochenodeoxycholate were significantly decreased in asthmatic patients compared with those in the COPD patients. Figure 6 shows the ROC curves evaluating the predictive performance of differential detection of metabolites with $AUC \geq 0.8$.

Altered Metabolic Pathways Analysis

By searching the KEGG database, the key

differential metabolites between the asthma patients and healthy controls were identified to be involved in the following pathways: purine metabolism, caffeine metabolism, tricarboxylic acid (TCA) cycle, protein digestion and absorption, and biosynthesis of amino acids (Figure 7). The key differential metabolites between asthma and COPD were identified to be involved in the pathways for purine metabolism and urea cycle (Figure 8).

DISCUSSION

Compared with other ‘-omics’ strategies, metabolomics can offer a number of advantages because of its close biological proximity to the phenotype of life systems and the rapid observation of system perturbations in the metabolome^[26]. A range of analytical platforms has been utilized in metabolic profiling studies, including chromatography coupled with MS or NMR spectroscopy, both of which are widely applied. For the first time, the present study demonstrated that the serum metabolic profiling of asthmatic patients was distinct from that of COPD and healthy subjects using UPLC-MS-based analysis. Our experimental data were of high quality and stability due to good QC. The QC samples were densely distributed in the PCA scatter 2D plots (refer to Supplementary Figures S1 and S2). Additionally, all the QC samples were within ± 2 standard deviation in the PCA scatter 1D plots (refer to Supplementary Figures S3 and S4 available in www.besjournal.com).

Initially, the present study further reinforced our previous findings, which showed that serum

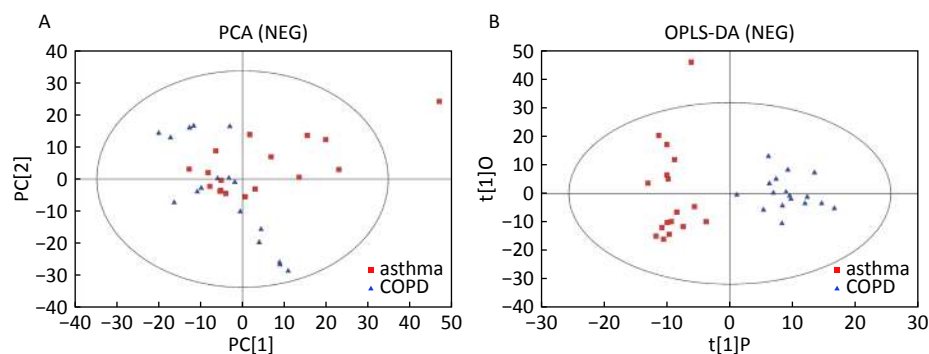


Figure 5. PCA and OPLS-DA of LC-MS metabolite profiles between asthma and COPD subjects in electrospray negative ion mode. (A) Score scatter plot of PCA model obtained from asthma and COPD subjects. The X-(PC[1]) and Y-axis (PC[2]) indicate the first and second principal components, respectively. (B) Score scatter plot of the OPLS-DA model obtained from asthmatic and COPD subjects. The X-(t[1]P) and Y-axis (t[1]O) indicate the predictive and orthogonal directions, respectively. PCA: principal component analysis; OPLS-DA: orthogonal projections to latent structures-discriminate analysis; LC-MS: liquid chromatography-mass spectrometry; COPD: chronic obstructive pulmonary disease.

metabolic profiling was significantly altered in patients with mild persistent asthma compared with that of healthy subjects based on GC-MS methods^[25]. In addition, several metabolites and their altered trends were highly similar between these studies. For example, we observed that in both studies, the levels of inosine increased, whereas those of L-glutamine and arachidonic acid decreased in asthmatic patients compared with those in healthy subjects. These studies could complement each other due to the presence of several high-molecular-

weight metabolites with poor thermal stability and which could only be detected by LC-MS methods^[26]. Notably, both R^2Y and Q^2Y scores in the OPLS-DA model exceeded 0.9, despite the application of the ESI mode (ESI+ or ESI-), suggesting that the models had excellent fitness and predictive power to distinguish asthmatic patients from healthy subjects.

A previous study conducted by Saude et al. revealed through NMR analysis that urine metabolites were associated with airway dysfunction in an ovalbumin-challenged animal model^[19]. They

Table 3. Differential detection of metabolites between asthmatic and COPD subjects

Metabolite name	Score	Median RT (s)	Mean asthma	Mean COPD	VIP	P-value	Fold-change ^a
Positive ion mode (ESI+)							
Hypoxanthine	0.888	127.044	762,120.978	381,909.931	2.527	0.001259746	1.996
Alpha-N-Phenylacetyl-L-glutamine	0.988	153.115	38,052.756	89,817.110	1.957	0.01036502	0.424
1-Methyladenosine	0.999	272.377	34,809.689	43,740.524	2.226	0.0038404	0.796
L-Pipecolic acid	0.963	236.526	232,104.868	123,058.269	1.738	0.01723709	1.886
P-chlorophenylalanine	0.946	299.633	103,213.840	88,268.687	1.065	0.02133749	1.169
Glycochenodeoxycholate	0.949	64.320	45,516.012	97,470.902	1.552	0.03594549	0.467
L-Citrulline	0.995	478.579	63,201.074	78,036.069	1.069	0.04906988	0.810
L-Glutamine	0.951	386.792	14,215.705	30,354.808	1.917	0.01095651	0.468
Acetylcarnitine	0.994	295.668	3,756,606.528	2,695,779.062	1.497	0.04943523	1.394
Negative ion mode (ESI-)							
Pseudouridine	0.983	210.311	103,185.823	150,318.467	2.984	0.000021522	0.686
Linoleic acid	0.819	48.449	385,935.752	265,424.563	1.472	0.04613066	1.454
Alpha-N-Phenylacetyl-L-glutamine	0.986	124.370	75,235.866	159,211.792	1.793	0.02703009	0.473
Hypoxanthine	0.986	127.177	421,202.385	228,230.660	2.046	0.00424504	1.846
Succinate	0.986	467.769	24,293.468	35,559.405	2.076	0.03407866	0.683
L-Citrulline	0.986	476.705	36,668.147	49,596.943	2.178	0.01640797	0.739
Glycochenodeoxycholate	1.000	63.258	111,864.373	232,527.155	1.661	0.04583166	0.481

Note. ^aFold-change: Asthma versus COPD. Abbreviations: RT: retention time; VIP: variable importance for the projection.

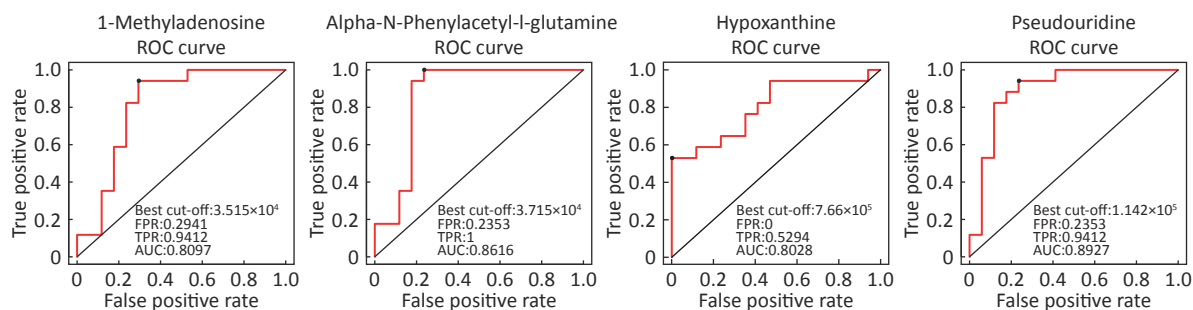


Figure 6. ROC curves of differential metabolites between asthmatic and COPD subjects with AUC \geq 0.80.

further utilized NMR analysis on urine samples to explore the differences in metabolite profiling among unstable asthmatic children, stable asthmatic children, and healthy subjects. The data indicated that urine metabolomic analysis could aid the identification of stable asthmatic patients from healthy subjects and of stable asthmatic patients from unstable asthmatic patients, achieving a good diagnostic accuracy (> 90%)^[20]. Subsequently, Mattarucchi et al. initially applied LC-MS analysis to urine samples in asthmatic children and healthy subjects and demonstrated that metabolite profiles were distinct between the asthmatic patients and control subjects. This finding was unaffected by asthma control and/or medication^[15]. Using a combined GC- and LC-MS platform, Ho et al. revealed that metabolite alterations in bronchoalveolar lavage fluid of ovalbumin-challenged mice could reverse several key metabolite changes compared with the levels of these metabolites in control animals and animals treated with glucocorticoids^[27]. In addition, several

experimental and human studies were conducted regarding metabolomic profiling differentiation between asthmatic patients and control subjects based on NMR methods and on different biofluid applications^[22-24,28]. Collectively, the data demonstrated that the systemic metabolic state in asthma was considerably different from that in healthy subjects, although different metabolites were identified among these studies.

Furthermore, our data indicated that serum metabolic profiling was different between mild asthma and stable COPD subjects. In a pilot study, metabolomic analysis of human urine samples based on NMR spectroscopy highlighted that metabolomic profiling differences could be noted between patients with asthma and those with COPD prior to and following exacerbation. In addition, their predictive model could diagnose blinded asthma and COPD correctly with optimal accuracy^[24]. However, the data regarding the application of metabolomic analysis on the differential diagnosis between asthma and COPD are still limited. Asthma and COPD

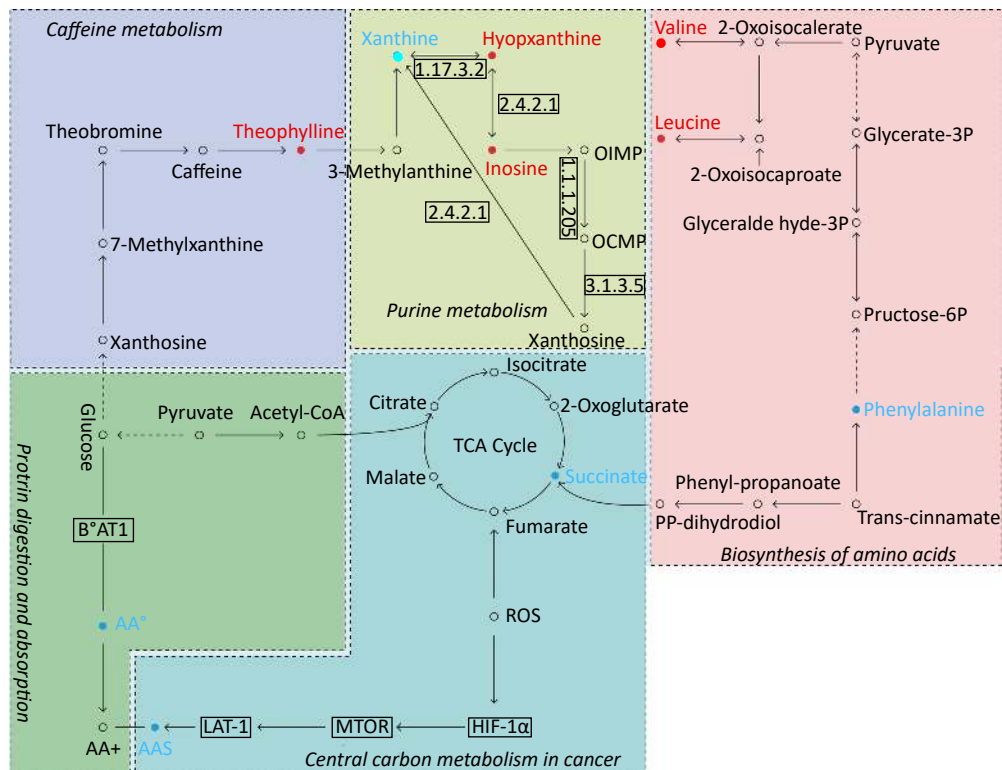


Figure 7. Pathway analysis of metabolomics alterations associated with asthmatic versus healthy control subjects. The purine metabolism, caffeine metabolism, TCA cycle, protein digestion and absorption, and biosynthesis of amino acids were altered in asthmatic subjects. Metabolite with red color in this reference map represents an increased level of this metabolite in asthmatic subjects, whereas the blue color represents a decrease.

are heterogeneous diseases with distinct phenotypes and in which metabolic states can differ from each other theoretically. The underlying mechanisms are unclear, and further studies are required to discover their precise function.

Notably, in our study, the OPLS-DA models for asthma and COPD exhibited no desirable predictive power compared with the models for asthma and healthy subjects. This finding was due to the Q^2Y values being lower than 0.5 (< 0.5) despite the optimal fitness of the models (R^2Y values were 0.879 for ESI+ mode and 0.901 for ESI- mode). These results may be ascribed to the following reasons: 1) The asthmatic and COPD subjects lacked matching in terms of age. The age is an important confounding factor for metabolic profiling analysis. 2) The patients with COPD were often current- or ex-smokers, and tobacco exposure may affect their metabolic profiles. 3) Relatively small sample sizes of asthma or COPD subject were used. Therefore, the differential detection of metabolites in the present study should be validated in a larger and prospective cohort study to assess their potential to distinguish asthma from COPD.

Interesting, the levels of hypoxanthine were evidently higher in asthmatic patients compared with those in healthy or COPD subjects. Hypoxanthine is a key metabolite in purine metabolism, and our study reported for the first time that the serum levels of hypoxanthine were significantly higher in asthmatic compared with healthy and/or COPD subjects. In addition, inosine is involved in purine metabolism, and its levels were significantly elevated in asthmatic patients compared with those in healthy subjects. Inosine can inhibit airway inflammation by reducing the number of macrophages, lymphocytes, and eosinophils, and cytokines interleukin-4 and -5 in the airway^[29]. The increased inosine level may be associated with the increased activity of adenosine deaminase (ADA), which converts adenosine to inosine. The increase in ADA activity can protect the body from the inflammation responses of bronchial asthma in animal models^[30]. We speculated that the increase in inosine is likely to be a protective response to airway inflammation in asthma. Purine metabolism is also proven to be associated with the pathogenesis of asthma in recent studies. Uric acid levels increased in

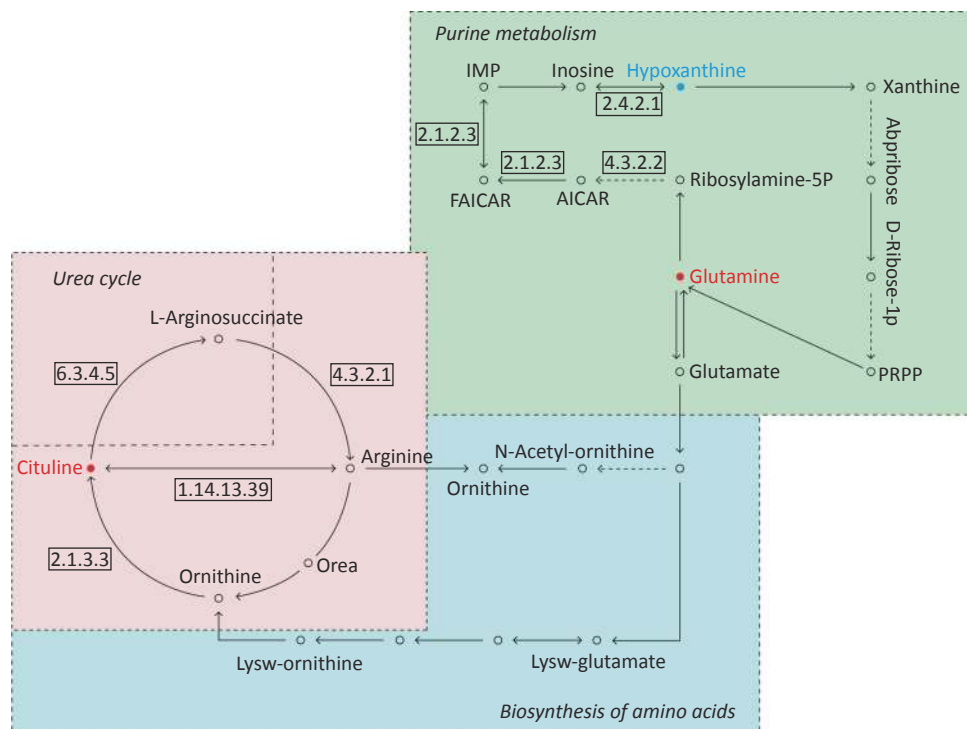


Figure 8. Pathway analysis of metabolomics alterations associated with asthmatic versus COPD subjects. The purine metabolism, urea cycle, and biosynthesis of amino acids were different between the two disorders. Metabolite with blue color in this reference map represents an increased level of this metabolite in asthmatic subjects, whereas the red color represents an increase of this metabolite in COPD subjects.

bronchoalveolar lavage fluid and pulmonary tissue homogenates in asthmatic patients and in asthmatic mouse models^[31]. Serum uric acid levels increased proportionally with the severity of asthma exacerbation and were inversely associated with lung function^[32]. Uric acid could be produced by human airway epithelial cells, and the level of extracellular uric acid in culture was elevated by allergen stimulation^[33]. An epidemiological study reported that the elevated serum uric acid level is a predictor for the development of airflow limitation^[34]. However, another study showed that plasma uric acid levels decreased in ovalbumin-challenged asthmatic mouse models^[35]. Although previous studies have shown inconsistencies, uric acid should be considered a useful biomarker for asthma. Uric acid is the final product of purine metabolism and is produced from xanthine and hypoxanthine by the enzyme xanthine oxidase. Therefore, the increasing levels of serum hypoxanthine in asthmatic patients in the present study suggests that xanthine oxidase may be inhibited, or hypoxanthine accumulates in the purine metabolic pathway in asthma, although no alteration of uric acid levels was detected in our study. According to our data, significantly increased serum hypoxanthine levels in asthma may aid the differential diagnosis of asthmatic patients compared with healthy individuals and COPD. Hypoxanthine can be a potential diagnostic biomarker for asthma. However, our study was a pilot research, and targeted metabolomic analysis should be conducted to further validate the role of hypoxanthine and purine metabolism in asthma.

In addition to purine metabolism, other metabolic pathways were identified to be involved in asthma. Metabolic alteration in TCA cycle had been identified and discussed in our previous work^[25]. Changes in amino acid metabolism could be observed in our study. The potential functions of these differential metabolites (i.e., L-valine, L-leucine, and L-phenylalanine) in asthma were unclear. In a recent metabolomics study, the urine levels of 3,4-dihydroxy-L-phenylalanine increased significantly in corticosteroid-nonrespondent children who had severe asthma compared with corticosteroid-respondent children^[36]. This finding was inconsistent to a certain extent with our study. In our research, the asthmatic subjects presented lower serum levels of L-phenylalanine than the healthy controls. However, the asthmatic subjects in our study comprised adults with mild asthma. The role of amino acid metabolism pathway in

development of asthma needs to be further studied in the future.

Compared with COPD subjects, in addition to purine metabolism, the pathways of urea cycle and arginine metabolism in asthmatic subjects differed. In bronchial epithelial cells, L-arginine is the substrate of nitric oxide synthase and the upstream metabolite of nitric oxide^[37]. The reduced bioavailability of L-arginine can limit the production of nitric oxide, and its bronchodilator effect will be impaired^[38]. L-Citrulline can be metabolized to L-arginine by the enzyme argininosuccinate^[39]. In our study, the serum levels of L-citrulline in asthmatic subjects were lower than that in COPD subjects, indicating that the bioactivity of argininosuccinate may differ between asthma and COPD, although no alteration in the levels of L-arginine was detected in our study. Another study showed that the whole-body citrulline rate of appearance was higher in stable COPD patients than in healthy controls, and the authors speculated that this phenomenon is likely a reflection of higher glutamine delivery and turnover because glutamine is the upstream metabolite of arginine^[40]. This finding can partly support our results because serum L-glutamine level was also elevated in COPD subjects, in addition to elevated serum L-citrulline levels, compared with asthmatic subjects. The metabolomic profile difference between asthma and COPD had also been identified in a recent study. COPD patients showed increased ethanol and methanol levels in their exhaled breath condensate and significantly lower levels of formate and acetone/acetoin compared with asthmatic patients^[41]. These findings reinforced the evidence indicating that airway inflammation is distinct between asthma and COPD.

The present study includes the following limitations: 1) Our results cannot be extrapolated to all the asthmatic patients and COPD subjects, as we only recruited individuals with mild persistent asthma and stable COPD. On the other hand, the association between metabolomic profiles and clinical phenotypes were excluded in the present study. This hypothesis can be tested in a study with a larger sample size. 2) The OPLS-DA models for asthma and COPD lacked a good predictive power, which has been mentioned previously. This finding may be due to the mismatched age and tobacco exposure between asthma and COPD subjects, which was the major limitation in our study. However, in clinical practice, individuals with COPD frequently include smokers and aged and exhibit lower incidence of allergic reactions compared with those

of subjects with asthma^[1,6]. Tobacco exposure was difficult to match between asthma and COPD patients. The diagnosis of COPD cannot be completely excluded in heavy smokers even when they exhibit typical asthma-like symptoms with variable airflow limitation. By contrast, a non-smoker with fixed airflow limitation should not be diagnosed as COPD indiscreetly.

Our LC-MS analysis demonstrated that individuals with asthma have a unique serum metabolome, which can be used to distinguish them from patients with COPD and healthy subjects. Purine metabolism alteration may be distinct and involved in the pathogenesis of asthma, as hypoxanthine serum levels are markedly elevated in asthmatic individuals.

COMPETING INTERESTS

The authors declare that they have no competing interests.

AUTHORS' CONTRIBUTIONS

LY and GXY analyzed and interpreted the patient data and was a major contributor in writing the manuscript. CC designed the study and collected and interpreted the patient data. ZX and WJ analyzed and interpreted the patient samples and revised the manuscript. TL contributed to the statistical analysis and interpreted the results. All authors read and approved the final manuscript.

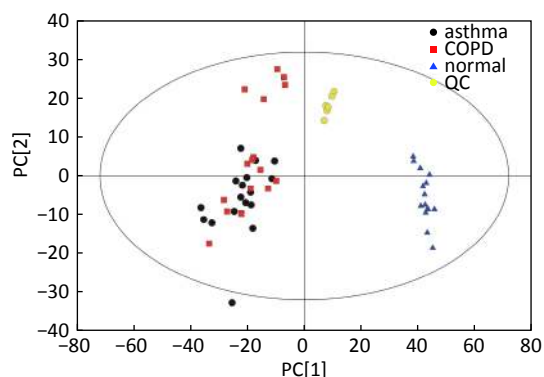
Received: March 3, 2019;

Accepted: September 2, 2019

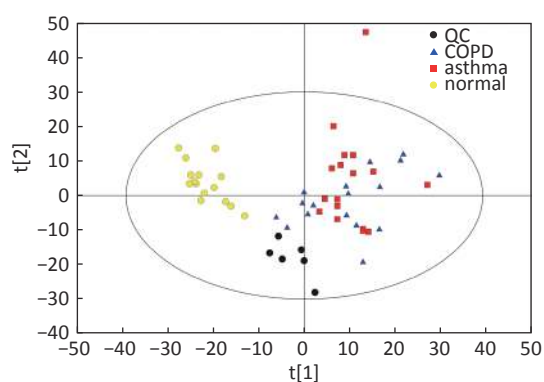
REFERENCES

- Global Strategy for Asthma Management and Prevention, Global Initiative for Asthma (GINA Updated 2017). <http://www.ginasthma.org/> [2017-5-14].
- Maniscalco M, Paris D, Melck DJ, et al. Coexistence of obesity and asthma determines a distinct respiratory metabolic phenotype. *J Allergy Clin Immunol*, 2017; 139, 1536–47.e5.
- Knuffman JE, Sorkness CA, Lemanske RF, et al. Phenotypic predictors of long-term response to inhaled corticosteroid and leukotriene modifier therapies in pediatric asthma. *J Allergy Clin Immunol*, 2009; 123, 411–6.
- Vital signs: asthma prevalence, disease characteristics, and self-management education: United States, 2001–2009. *MMWR Morb Mortal Wkly Rep*, 2011; 60, 547–52.
- Zhang ZL, Wang J, Liu F, et al. Circulating Neutrophil Counts Decrease in Response to Mitigated Air Quality in Stable COPD Patients. *Biomed Environ Sci*, 2018; 31, 66–71.
- Global Strategy for the Diagnosis, Management and Prevention of Chronic Obstructive Pulmonary Disease, Global Initiative for Chronic Obstructive Lung Disease (GOLD) 2017. Available from: <http://www.goldcopd.org/> [2017-4-20].
- Menezes AM, de Oca MM, Pérez-Padilla R, et al. Increased risk of exacerbation and hospitalization in subjects with an overlap phenotype: COPD-asthma. *Chest*, 2014; 145, 297–304.
- Sethi S, Mahler DA, Marcus P, et al. Inflammation in COPD: implications for management. *Am J Med*, 2012; 125, 1162–70.
- Hogg JC. Pathophysiology of airflow limitation in chronic obstructive pulmonary disease. *Lancet*, 2004; 364, 709–21.
- Snowden S, Dahlén SE, Wheelock CE. Application of metabolomics approaches to the study of respiratory diseases. *Bioanalysis*, 2012; 4, 2265–90.
- Zhou B, Xiao JF, Tuli L, et al. LC-MS-based metabolomics. *Mol Biosyst*, 2012; 8, 470–81.
- Arakaki AK, Skolnick J, McDonald JF. Marker metabolites can be therapeutic targets as well. *Nature*, 2008; 456, 443.
- Nobakht MGBF, Aliannejad R, Rezaei-Tavirani M, et al. The metabolomics of airway diseases, including COPD, asthma and cystic fibrosis. *Biomarkers*, 2015; 20, 5–16.
- Dallinga JW, Robroeks CM, van Berkel JJ, et al. Volatile organic compounds in exhaled breath as a diagnostic tool for asthma in children. *Clin Exp Allergy*, 2010; 40, 68–76.
- Mattarucchi E, Baraldi E, Guillou C. Metabolomics applied to urine samples in childhood asthma; differentiation between asthma phenotypes and identification of relevant metabolites. *Biomed Chromatogr*, 2012; 26, 89–94.
- Gahleitner F, Guallar-Hoyas C, Beardsmore CS, et al. Metabolomics pilot study to identify volatile organic compound markers of childhood asthma in exhaled breath. *Bioanalysis*, 2013; 5, 2239–47.
- Comhair SA, McDunn J, Bennett C, et al. Metabolomic Endotype of Asthma. *J Immunol*, 2015; 195, 643–50.
- Carraro S, Rezzi S, Reniero F, et al. Metabolomics applied to exhaled breath condensate in childhood asthma. *Am J Respir Crit Care Med*, 2007; 175, 986–90.
- Saude EJ, Obiefuna IP, Somorjai RL, et al. Metabolomic biomarkers in a model of asthma exacerbation: urine nuclear magnetic resonance. *Am J Respir Crit Care Med*, 2009; 179, 25–34.
- Saude EJ, Skappak CD, Regush S, et al. Metabolomic profiling of asthma: diagnostic utility of urine nuclear magnetic resonance spectroscopy. *J Allergy Clin Immunol*, 2011; 127, 757–64.
- Ibrahim B, Marsden P, Smith JA, et al. Breath metabolomic profiling by nuclear magnetic resonance spectroscopy in asthma. *Allergy*, 2013; 68, 1050–6.
- Jung J, Kim SH, Lee HS, et al. Serum metabolomics reveals pathways and biomarkers associated with asthma pathogenesis. *Clin Exp Allergy*, 2013; 43, 425–33.
- Motta A, Paris D, D'Amato M, et al. NMR metabolomic analysis of exhaled breath condensate of asthmatic patients at two different temperatures. *J Proteome Res*, 2014; 13, 6107–20.
- Adamko DJ, Nair P, Mayers I, et al. Metabolomic profiling of asthma and chronic obstructive pulmonary disease: A pilot study differentiating diseases. *J Allergy Clin Immunol*, 2015; 136, 571–580.e3.
- Chang C, Guo ZG, He B, et al. Metabolic alterations in the sera of Chinese patients with mild persistent asthma: a GC-MS-based metabolomics analysis. *Acta Pharmacol Sin*, 2015; 36, 1356–66.
- Dunn WB, Broadhurst D, Begley P, et al. Procedures for large-scale metabolic profiling of serum and plasma using gas chromatography and liquid chromatography coupled to mass spectrometry. *Nat Protoc*, 2011; 6, 1060–83.
- Ho WE, Xu YJ, Xu F, et al. Metabolomics reveals altered metabolic pathways in experimental asthma. *Am J Respir Cell Mol Biol*, 2013; 48, 204–11.

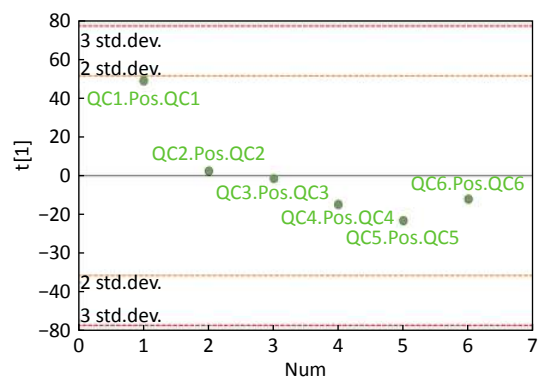
28. Quan-Jun Y, Jian-Ping Z, Jian-Hua Z, et al. Distinct Metabolic Profile of Inhaled Budesonide and Salbutamol in Asthmatic Children during Acute Exacerbation. *Basic Clin Pharmacol Toxicol*, 2017; 120, 303–311.
29. da Rocha Lapa F, de Oliveira APL, Accerruri BG, et al. Anti-inflammatory effects of inosine in allergic lung inflammation in mice: evidence for the participation of adenosine A2A and A3 receptors. *Purinergic Signal*, 2013; 9, 325–36.
30. Trevelthick MA, Mantell SJ, Stuart EF, et al. Treating lung inflammation with agonists of the adenosine A2A receptor: promises, problems and potential solutions. *Br J Pharmacol*, 2008; 155, 463–74.
31. Kool M, Willart MA, van Nimwegen M, et al. An unexpected role for uric acid as an inducer of T helper 2 cell immunity to inhaled antigens and inflammatory mediator of allergic asthma. *Immunity*, 2011; 34, 527–40.
32. Li L, Wan C, Wen F. An unexpected role for serum uric acid as a biomarker for severity of asthma exacerbation. *Asian Pac J Allergy Immunol*, 2014; 32, 93–9.
33. Huff RD, Hsu AC, Nichol KS, et al. Regulation of xanthine dehydrogenase gene expression and uric acid production in human airway epithelial cells. *PLoS One*, 2017; 12, e0184260.
34. Fukuhara A, Saito J, Sato S, et al. The association between risk of airflow limitation and serum uric acid measured at medical health check-ups. *Int J Chron Obstruct Pulmon Dis*, 2017; 12, 1213–9.
35. Yu M, Cui FX, Jia HM, et al. Aberrant purine metabolism in allergic asthma revealed by plasma metabolomics. *J Pharm Biomed Anal*, 2016; 120, 181–9.
36. Park YH, Fitzpatrick AM, Medriano CA, et al. High-resolution metabolomics to identify urine biomarkers in corticosteroid-resistant asthmatic children. *J Allergy Clin Immunol*, 2017; 139, 1518–24.e4.
37. Lane C, Knight D, Burgess S, et al. Epithelial inducible nitric oxide synthase activity is the major determinant of nitric oxide concentration in exhaled breath. *Thorax*, 2004; 59, 757–60.
38. Morris CR, Poljakovic M, Lavrisha L, et al. Decreased arginine bioavailability and increased serum arginase activity in asthma. *Am J Respir Crit Care Med*, 2004; 170, 148–53.
39. Winnica D, Que LG, Baffi C, et al. L-citrulline prevents asymmetric dimethylarginine-mediated reductions in nitric oxide and nitrosative stress in primary human airway epithelial cells. *Clin Exp Allergy*, 2017; 47, 190–9.
40. Jonker R, Deutz NE, Erbland ML, et al. Alterations in whole-body arginine metabolism in chronic obstructive pulmonary disease. *Am J Clin Nutr*, 2016; 103, 1458–64.
41. Maniscalco M, Paris D, Melck DJ, et al. Differential diagnosis between newly diagnosed asthma and COPD using exhaled breath condensate metabolomics: a pilot study. *Eur Respir J*, 2018, 51.



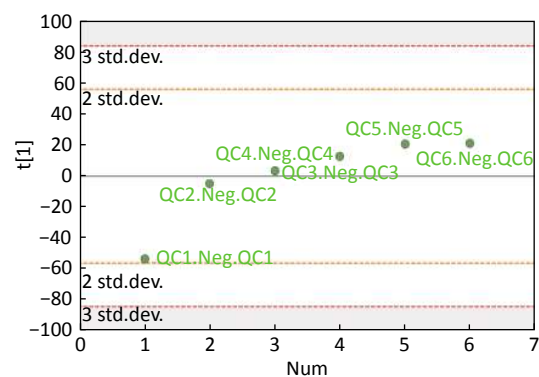
Supplementary Figure S1. Distribution of QC samples in PCA scatter 2D plots (Supplementary Figures S1 and S2 for ESI+ and ESI- mode, respectively). QC samples were densely distributed in these plots (yellow points in ESI+ mode and black points in ESI- mode).



Supplementary Figure S2. Distribution of QC samples in PCA scatter 2D plots (Supplementary Figures S1 and S2 for ESI+ and ESI- mode, respectively). QC samples were densely distributed in these plots (yellow points in ESI+ mode and black points in ESI- mode).



Supplementary Figure S3. QC samples in PCA scatter 1D plots (Supplementary Figures S3 and S4 for ESI+ and ESI- mode, respectively). All of the QC samples were within the 95% confidential interval and ± 2 standard deviation.



Supplementary Figure S4. QC samples in PCA scatter 1D plots (Supplementary Figures S3 and S4 for ESI+ and ESI- mode, respectively). All of the QC samples were within the 95% confidential interval and ± 2 standard deviation. Abbreviations: PCA: principal component analysis; ESI: electrospray ionization source; QC: quality control.

Supplementary Table S1. Gradient elution program used in Ultra Performance Liquid Chromatography method

Time (min)	Flow rate ($\mu\text{L}/\text{min}$)	Mobile phase A (%)	Mobile phase B (%)
0.00	300	15	85
1.00	300	15	85
12.00	300	35	65
12.10	300	60	40
15.00	300	60	40
15.10	300	15	85
20.00	300	15	85

Mobile phase A: water containing 25 mM ammonium acetate and 25 mM ammonium hydroxide; Mobile phase B: acetonitrile